General Disclaimer

One or more of the Following Statements may affect this Document

- This document has been reproduced from the best copy furnished by the organizational source. It is being released in the interest of making available as much information as possible.

- This document may contain data, which exceeds the sheet parameters. It was furnished in this condition by the organizational source and is the best copy available.

- This document may contain tone-on-tone or color graphs, charts and/or pictures, which have been reproduced in black and white.

- This document is paginated as submitted by the original source.

- Portions of this document are not fully legible due to the historical nature of some of the material. However, it is the best reproduction available from the original submission.

Produced by the NASA Center for Aerospace Information (CASI)

QUARTERLY REPORT NO. 2
CONTRACT JPL 952129

HUGHES

HUGHES AIRCRAFT COMPANY

ION ENGINE THRUST VECTOR STUDY

APRIL 1969

HUGHES RESEARCH LABORATORIES · MALIBU

HUGHES RESEARCH LABORATORIES
Malibu, California

a division of hughes aircraft company

ION ENGINE THRUST VECTOR STUDY

Quarterly Report No. 2
JPL Contract 952129

Prepared by

S. Kami, W.G. Herron, and H. King

April 1969

TABLE OF CONTENTS

LIST OF ILLUSTRATIONS

ABSTRACT

This report describes the detail design and fabrication of the thrust stand and the 30 cm thruster. It includes results of tests performed on single components and also on component systems. Analysis of the effect of external environmental vibration on the thrust vector measurement accuracy is also included. A mechanically isolated vacuum chamber is shown in its preliminary planning stage. Thruster tests were performed and results described.

I. INTRODUCTION AND SUMMARY

The "floating" thrust stand described in the previous quarterly report was designed in detail during this period, and fabrication was begun. Because of the low force level (10^{-4} lb) to be measured with this thrust stand, the electrical leads which will be used between the fixed and the floating portion of the stand have received special attention. The spring rates of several configurations of flexible cabling have been tested, and a photoelectric sensor has been devised for detecting the motion of the floating platform from its "null" (and thus balanced) position. Electromagnetic force motors similar to loudspeaker voice coils have been designed and fabricated to provide the necessary force to return the thrust stand to the null position. Circuitry for detecting the position change of the sensor and driving the force motor has been designed and breadboarded, and the loop has been tested for response, sensitivity, and linearity.

A vibration survey was performed to determine the vibration level in the 9 ft vacuum test chamber; the results indicate that the acceleration level is on the order of 3×10^{-3} g at a frequency of 25 Hz at the center of the chamber. Depending on the platform structural rigidity, this frequency vibration or some harmonic could be transmitted to the thrust stand and cause background noise. One solution is to mount the thrust stand on rubber pneumatic vibration isolators with resonance frequencies of approximately 1.5 Hz to insure the removal of chamber transmitted vibration problems. A high priority program is now proceeding to set a 4 ft chamber upright and install rubber-pneumatic vibration isolators with less than the 1.5 Hz resonance frequency. Present estimates indicate that 60 days will be required to complete the task. This estimate is compatible with the program schedule for the start of thrust stand and thruster integration.

An oxide cathode 30 cm thruster has been designed and fabricated. The electrodes incorporate a center support; the outer supports for the accel electrode are normally mounted from the screen electrode on dual leaf spring assemblies which allow differential thermal growth of the electrodes without imposing a large bending moment on the screen electrode. The supports were designed for use on thrust stand tests of the thruster with axial, lateral, and radial displacements imposed. The displacements will be caused by mechanisms driven by a solenoid actuated stepping motor device. On the thrust stand the accel electrode will be mounted through the outer supports on a plate which is a part of the thruster mounting plate. One stepping motor will cause the plate to move axially, another will cause tilting, a third will cause the electrode to rotate, and a fourth will cause lateral motion. Tests performed on commercial stepping motors show that with minor modification they will provide sufficient operating torque and reliability to actuate these mechanisms.
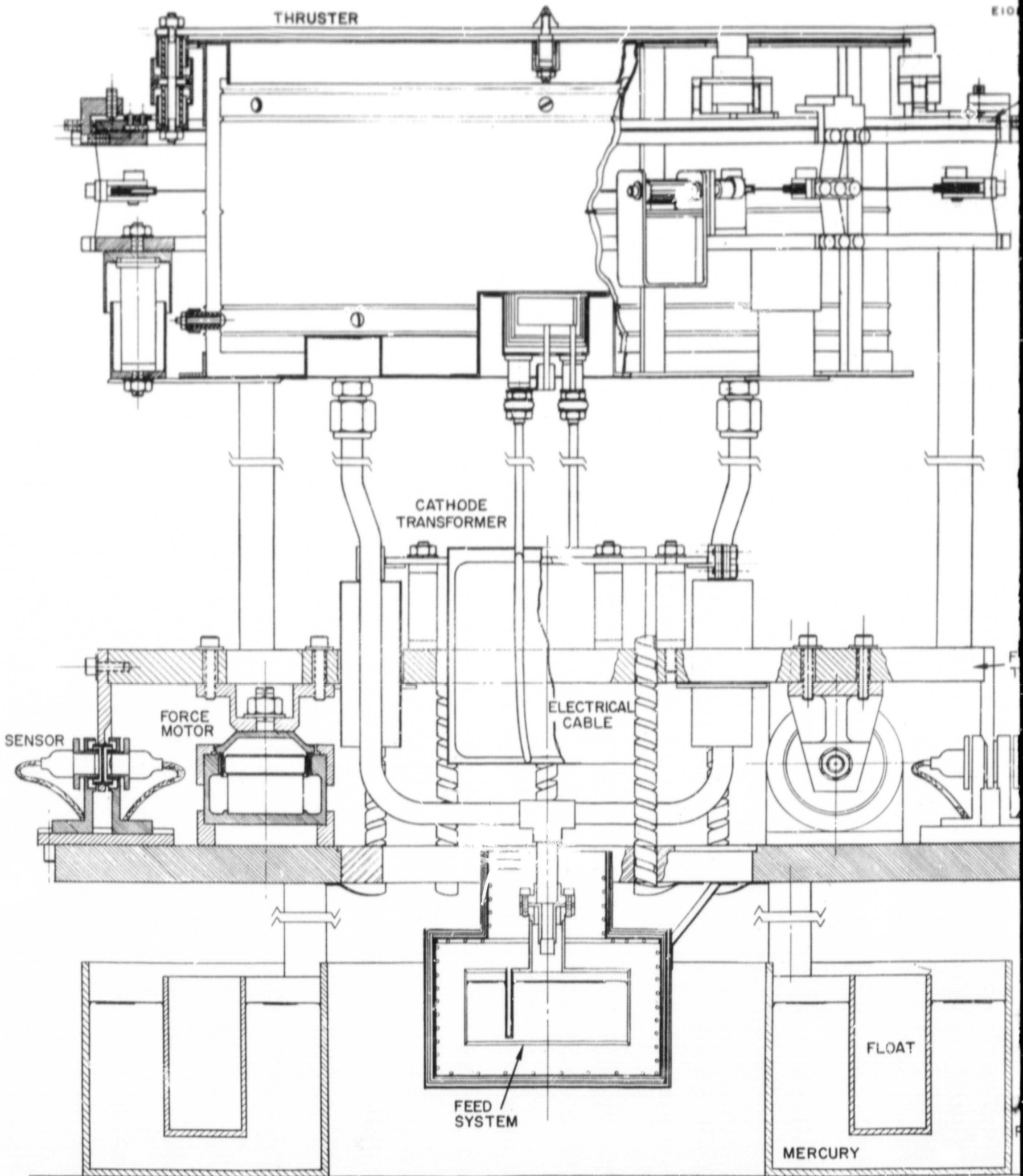
2

II. THRUST STAND DESIGN

The thrust stand design concept and analysis were discussed in the previous quarterly report. Force motor and electronic system requirements were determined on the basis of the analysis and estimated weights at the start of this program. Because of functional considerations the thruster was located on the top, with the thrust directed upward. The center section contains the force motor and sensors; this is the preferred orientation because these components should be near the center of gravity. The thrust stand assembly with the thruster mounted on it is shown in Fig. 1.

A. Float

The float is an open top cylindrical ring of U-shaped cross section. Its volume is such that it will support 28.8 lb/in. of immersion in mercury. The pan or container for the mercury is also a U cross section to allow a central passage for electrical leads and to provide a well for the thruster feed system reservoir. The clearance between the float and the pan walls is 1-3/8 in. at the surface of the mercury in order to minimize surface tension effects (which may result from the liquid-solid interfaces if mercury should adhere to the float and pan walls). In order to inhibit the adherence of mercury, the contacting surfaces of both the pan and float have been coated with teflon.

B. Electrical Conductor Cables

A commercially available electrical cable with insulation capable of withstanding the high voltage and sufficient flexibility for this application was obtained from Cicoil Corp. of Chatsworth upon the recommendation of the R&D Division of Hughes Aircraft. The R&D Division also produces a flexible cable which is lighter than that produced by the Cicoil Corp.; however, it was not recommended because of its limited current carrying capacity and because this contract requires omnidirectional flexibility of the cable.

THRUSTER

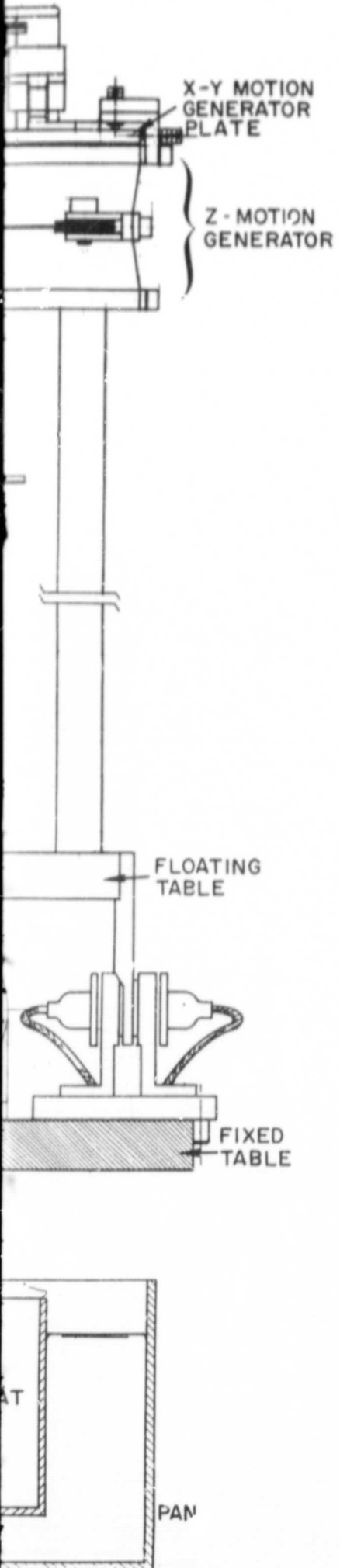CATHODE
TRANSFORMER

SENSOR

FORCE
MOTOR

ELECTRICAL
CABLE

FEED
SYSTEM

FLOAT

MERCURY

4

E1080-12

X-Y MOTION
GENERATOR
PLATE

{ Z - MOTION
GENERATOR

Fig. 1.   Thrust stand assembly.

FLOATING
TABLE

FIXED
TABLE

AT

PAN

A test fixture has been fabricated for measuring the low forces, such as the resistance to flexing of the electrical cables between the fixed and the floating portion of the thrust stand. The test fixture is a one degree of freedom air bearing consisting of a triangular cross section plenum perforated on two surfaces with many small holes and a slider which fits closely over the perforated surfaces. Pressurizing the plenum with air or nitrogen causes the slide to lift, and a virtually friction free system results. Tilting the plenum will cause the slide to move to the lower end of the plenum. With no restraints the amount of tilt required to start the slide moving is less than 0.0005 in. on the 12 in. long plenum. The motion of the slide is detected by the optical sensor designed and reported during Phase I of this program. With the sensor electronic circuitry employed at present, a sensitivity of 0.0018 in. per 100 mA is obtained. With a slide weight of 250 g, including the sensor aperture, counterweights, and half of the cable weight, it is possible to determine the spring rate of the cable by measuring the displacement of the slide as the air bearing plenum is tilted through a few degrees of arc from the following:

$$k = \frac{W \cdot \Delta h}{L \cdot \zeta \cdot 454}$$

where

$k \equiv$ spring rate of the cable, pounds per inch

$W \equiv$ weight of the slide, grams

$\Delta h \equiv$ displacement of the airbearing plenum on one end, inch

$L \equiv$ length of the plenum between pivot and micrometer tilt mechanism, inches

$\zeta \equiv$ displacement of the slide from null to equilibrium with Wh/L force.

A test of two cables with opposing 90° twists indicates that this cable configuration results in a spring rate of 0.05 lb/in. Because the thrust stand at null will remain well within 0.0005 in. of its initial position, the forces from the leads will be

$$F < (5 \times 10^{-2} \text{ lb/in.}) (5 \times 10^{-4} \text{ in.}) (8 \text{ leads}) = 2 \times 10^{-4} \text{ lb,}$$

which is comparable to the force to be measured.

Several conductor cable configurations have been tested during this period, with the results shown in Table I. Because the cable must be able to move freely in all three axes, the looped cable is the most desirable configuration. The direction sensitivity shown between tests 8c and 9 is undesirable. It was thought that splitting the insulation between conductors, as in test 4, would reduce the effective "web" thickness and result in a direction insensitive flexible cable; however, the test results do not support this assumption. These show instead an inconsistent spring rate which at present is attributed to the random rubbing of the strands against each other.

A helically wound cable configuration would result in a low spring rate and be insensitive to direction. The supplier of the cable was not able to provide specific instructions for coiling or forming the cables. Long duration immersion of coiled cable in solvents (such as acetone, alcohol, or trichlorethylene) or heating at 260°C were suggested as possible means of setting the cable. Further investigation suggested the possibility of chemical catalyst and sulfur vulcanization at the temperatures of the previous air firing.[1,2] The first method tried was to immerse the cable in methyl-ethyl-ketone (MEK) after heating at 280°C for 30 min and then reheat to 280°C to drive out the MEK. In one case the coiled cable had a small spring-back when released from the mandrel. A second trial resulted in blistering of the insulation. Sulfur vulcanization by sprinkling flowers of sulfur directly on the coiled cable caused the cable to adhere to the mandrel.

TABLE I

Electrical Cable Test

	TEST NUMBER	L (INCHES)	THICKNESS t (INCHES)	WIDTH b (INCHES)
	1	1.86	.034 (.260)	.260 (.034)
	3	1.86	.034 (.260)	.260 (.034)
	2	1.86	.034	.260
	2A	1.86	.034	.260
LEAD SPLIT BETWEEN CONDUCTORS	4	1.86	.260	.034
	5	1.86	.260	.034
	6	3.75	.034	.260
	6A	3.75	.034	.260
MOLDED SILICONE	7	.70	.034 (.260)	.260 (.034)
	12	1.70	.034 (.260)	.260 (.034)
$L_1 = 3.11"$ TOTAL LEAD L = 4.38"	8A	4.38	.034	.260
SAME AS ABOVE EXCEPT $L_1 = 3.61"$	8B	4.38	.034	.260
SAME AS ABOVE EXCEPT $L_1 = 4.11"$	8C	4.38	.034	.260
SAME AS TEST 8C EXCEPT MOTION 90° FROM THAT SHOWN	9	4.38	.034	.260
SAME AS TEST 8A EXCEPT MOTION 90° FROM THAT SHOWN	9A	4.38	.034	.260

TABLE I

Electrical Cable Test Results

THICKNESS t(inches)	WIDTH b(inches)	SPRING CONSTANT K ($\frac{LBS}{IN}$)	MODULUS OF ELASTICITY E (PSI)	REMARKS
(.260)	.260(.034)	.42	1.45×10^5	
(.260)	.260(.034)	.48	1.66×10^5	LEADS DIFFERENT THAN TEST 1
	.266	.046	1.16×10^5	
	.260	.039	1.0×10^5	LEADS DIFFERENT THAN TEST 2
	.034	≈.65		SPRING RATE NONLINEAR – INCONSISTANT
	.034	≈3.4	1.47×10^5	SPRING RATE NONLINEAR
	.260	-.062	$.8 \times 10^5$	
	.260	-.062	$.8 \times 10^5$	
(.260)	.260(.034)	.268		ONE LEAD ONLY
(.260)	.260(.034)	.163		SAME AS TEST 7 EXCEPT 1" ADDED TO ENDS
	.260	-.036		
	.260	-.029		
	.260	-.010		
	.260	.290		
	.260	.265		

Heat aging of the cable at 260^OC in air yielded the most consistent results. Several samples were prepared and aged for varying lengths of time. The best results were obtained after a 4 hour aging period; shorter aging resulted in partially set coils, and longer aging caused the insulation to adhere to the mandrel and to soften and tear readily.

The 4 hour sample retained its resilience while holding the coil "set." It could be stretched 50 to 60% and bent 45 to 60° without losing its set; stretching or bending beyond these limits causes deformation.

Tests of the helically coiled cables with the coil ends clamped perpendicular to the wires show that the spring rate of this configuration is not direction sensitive and is 0.051 lb/in., which is slightly greater than the spring rate of the cable in the direction perpendicular to its width.

Close inspection of the coiled cable movement while it was clamped as described above revealed that although five turns of cable were held in the space between the two clamps, most (70 to 80%) of the flexing occurred within the turns adjacent to the clamps. A fixture is now being prepared for holding at least one turn of the cable; the helically formed cable will be installed in a cylinder and clamped against the walls by means of an expanding cylindrical spring from within the helix. This device should impart a stiffness to the first free turn, which would cause all of the turns in the cable to be flexed equally and result in a lower spring rate.

C.   Force Motors

The force motor design goal was 1/2 lb of force for an input of 1/4 A at 15 V. The thrust stand analysis indicated that a force of 0.1 lb would be adequate, and that the higher force capability of the force motor would enhance the response of the system. The force motor design is similar to that of a voice coil of a loudspeaker except for the air gap. In a normal loudspeaker the air gap is very small and

the coil is usually a wire on a thin backing of paper. The coil is centered on the airgap by a diaphragm or a flat spring. The force motor must be capable of accommodating both axial and lateral displacement, and thus by necessity has a larger air gap than the loudspeaker voice coil. The effect of this large air gap is then a significant increase in the flux leakage at the air gap.

A design flux density of 2000 G was assumed for a 0.25 in. air gap of the magnetic circuit. A coil diameter of 1.50 in. was selected based on the flux of Alnico V and the size of readily available plug magnets. The coil width of 0.375 in. was selected to overlap the pole faces of 0.313 in. by 10% on each side. The 0.313 in. pole face width at 1.438 in. diameter matches the cross sectional area of the plug magnet. Similar area matches were made throughout the iron. The magnet assembly is 2-1/2 in. in diameter and 1-1/2 in. high.

Initial tests of the force motor showed a force of 0.13 lb at 300 mA. The magnet was magnetized in situ and a nearly four-fold increase in the force, to 0.5 lb at 300 mA, was realized.

A z axis force motor assembly is shown in Fig. 2. The x-y force motors are identical to that shown, except for the mounting. The z force motors are mounted with their axes vertical and the line of force is in the vertical direction. The x-y force motors are mounted with their axes horizontal; the axes of the two x force motors are perpendicular to those of the two y force motors.

A guide ring is pressed on the body of the magnet assembly. The mount of the coil assembly has a machined shoulder which overhangs the coil and fits within the guide ring of the magnet. The clearance between the diameter of the shoulder and the guide ring is 0.031 in. and that between the coil and the magnet pole faces is 0.040 in. Thus the guide-shoulder acts to protect the coil by stopping motion. It is also intended as an aid in the installation of the force motor during thrust stand assembly. The force motors must be positioned on the tables as an assembly. If a 0.03 in. thick split ring is placed in the
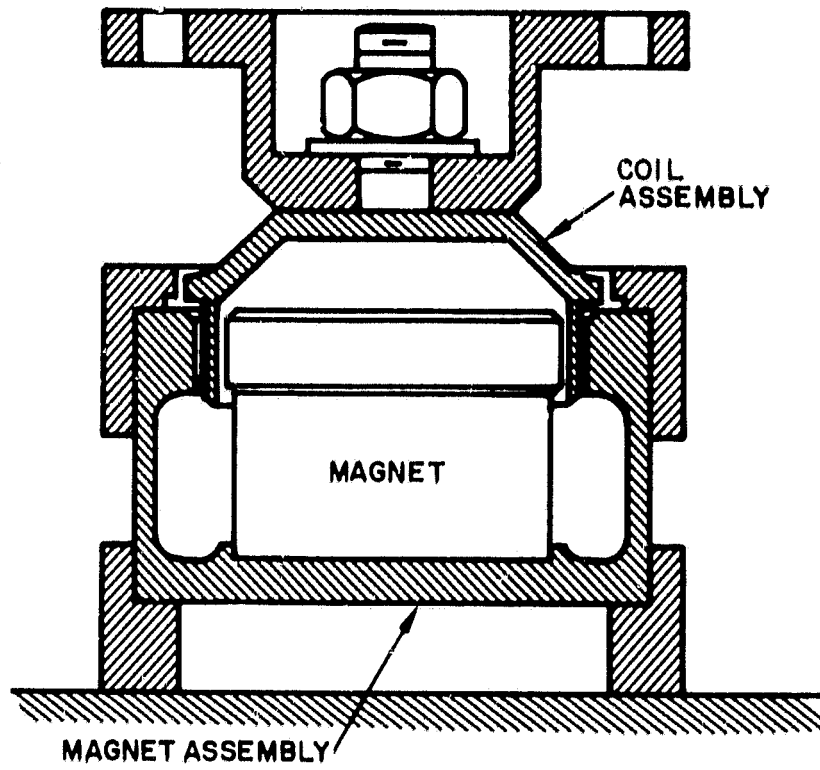
Fig. 2. Axial force motor assembly.

clearance between the shoulder and guide ring and 0.031 in. pins are placed through four holes in the guide rings to maintain the spacing between the bottom of the shoulder and the top of the magnet sub-assembly, the force motor assembly is in the null position. The split ring and spacer pins should be left in place until all of the force motors are in position.

D.   Photoelectric Displacement Sensor

The displacement sensor described in the previous quarterly report will be used as designed. Some mounting modifications were made to the original design to fit the later thrust stand design. Several tests made of the sensors verify the preliminary results reported earlier.

E.   Sensor-Force Motor Electronics

The proposed electronic control loop configurations were discussed in the previous quarterly report, and a detailed analysis (paper study and analog simulation) of the expected system performance was presented. The major effort during this quarter has been directed toward (1) hardware implementation and testing of electronics for a single control loop; (2) design and layout of the total electronic subsystem (control and instrumentation); and (3) procuring components.

The electronics for the single control loop, which was constructed and tested, is shown in Fig. 3. The component values and the amplifiers indicated are those suggested (as nominal) for each of the eight control loops to be used in the final system.

Although no completely realistic model was available of the actual dynamic load which the force motor will drive in the final system, various closed loop tests were performed using the electronics of Fig. 3 and the mechanical setup shown in Fig. 4. The tests were intended to determine qualitatively the compatibility of components, the ease of compensation adjustments and their relative effects, the procedure for simultaneous mechanical and electrical null adjustments, etc.

14

Fig. 3.   Electronics for a single control loop.

W

W   ΔW ← DIFFERENTIAL
WEIGHT TO
BE MEASURED

BALANCE

UNIVERSAL
JOINT→

AIR BEARING SUPPORT

MOTION SENSOR APERTURE

MOTION SENSOR DETECTOR
(LIGHT SOURCE NOT SHOWN)

FORCE MOTOR
COIL

COIL
LEADS

FORCE MOTOR
MAGNET ASS'Y →

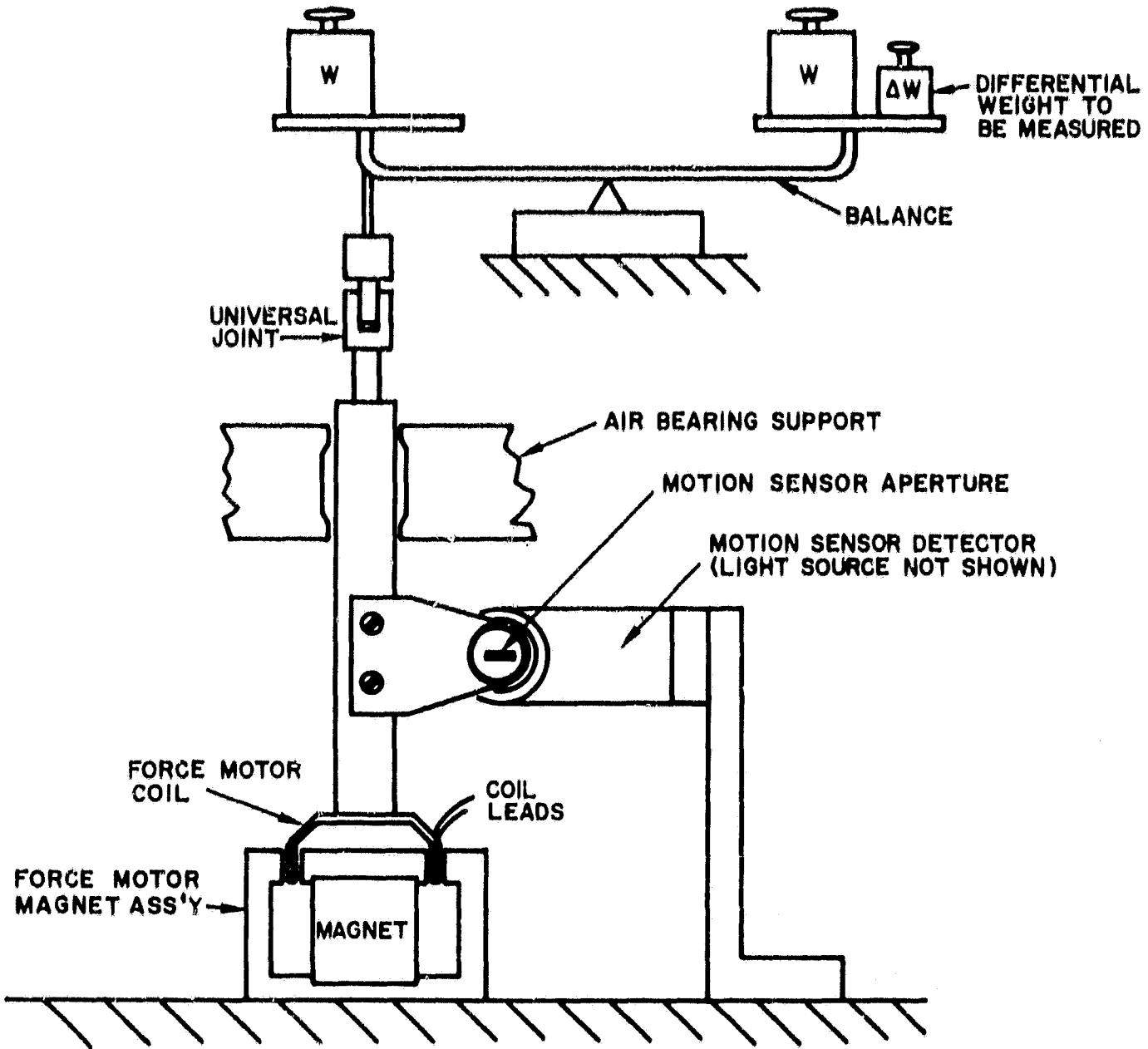MAGNET
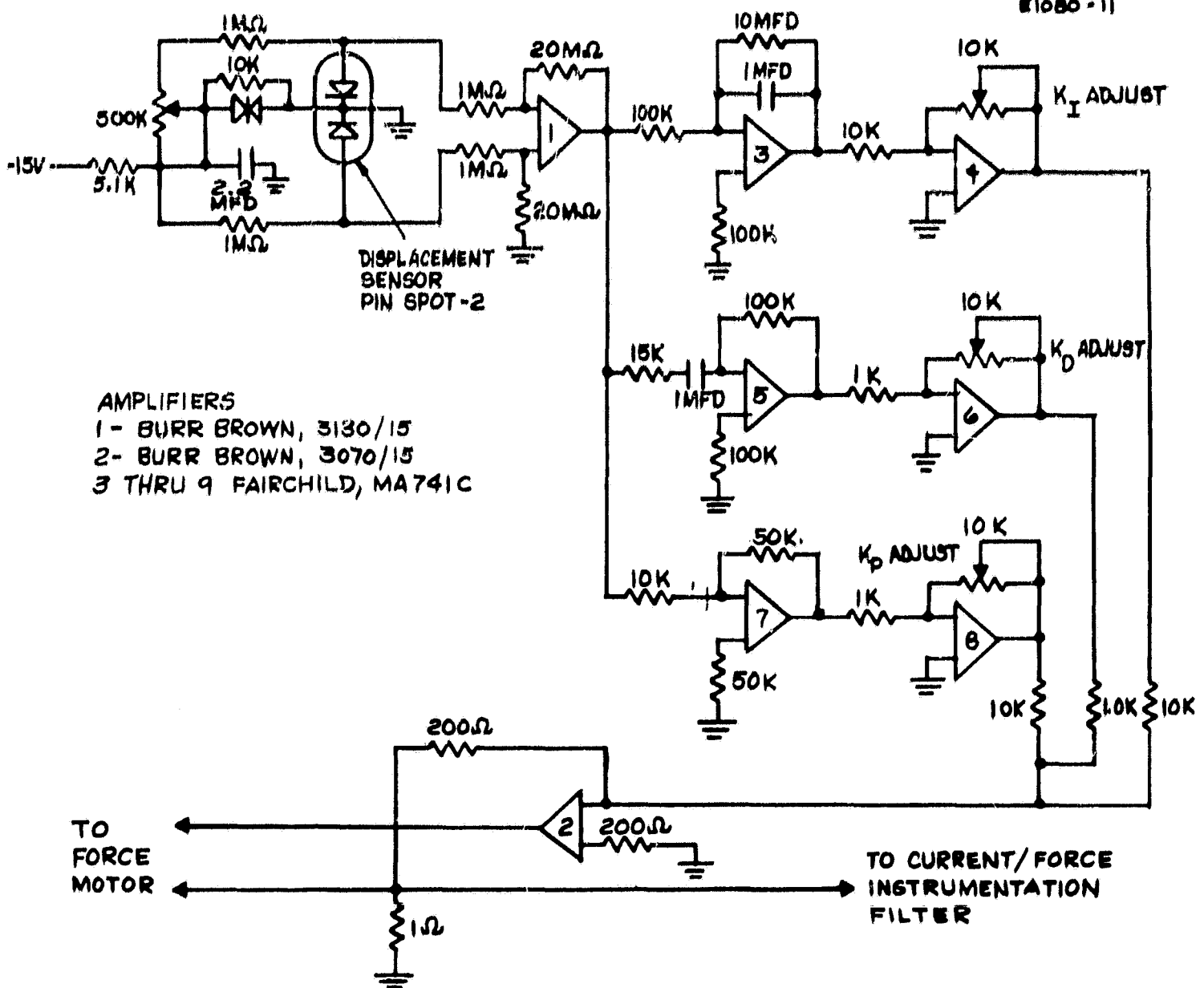
Fig. 4.   Closed loop mechanical test setup.

The adjustable compensation gain constants functioned as expected. The loop was unstable with only position information and became stable as the derivative (rate) compensation was increased. Error displacement could be driven to essentially zero (zero average value) by providing a signal which is proportional to the integral of the error. With all gain constants (K_p, K_d, K_I) adjusted to apparently satisfactory values for reasonably well damped transient response, no electrical zero drift was detected over a period of approximately 6 hours at ambient room temperature.

The indicated displacement noise (due to vibration of the building, etc.) was approximately 30 MV peak-to-peak (at the output of the sensor electronics) and corresponds to a displacement of ± 25 μin. It is of more importance that in this particular test setup the background vibration produced a force motor current variation equivalent to approximately ± 5 mlb. The wave shape at the sensor tended to be sinusoidal (in the frequency range of 30 to 60 Hz) and the amplitude was dependent on the total weight placed on the balance, decreasing with an increase in weight. It should be emphasized that this sinusoidal displacement had very little effect on the indicated differential force when read on a current meter with slow response. A static differential force in the range of 10^{-4} lb could be accurately determined. Based on the above and other pertinent information on the expected vibrational effects, a low pass filter will be incorporated in the current/force instrumentation.

F.   Vibration

With the aid of a very simplified model, the relationship between the vibrational displacement of the base of the thrust stand and the restoring force motor drive current will be discussed.

The simplified model to be used is shown in Fig. 5. In this single degree of translation model, X_1 represents the position of the outer housing of the thrust stand (termed the pan) located on a vibrating structure and X_2 is the relative position (with respect to a fixed reference
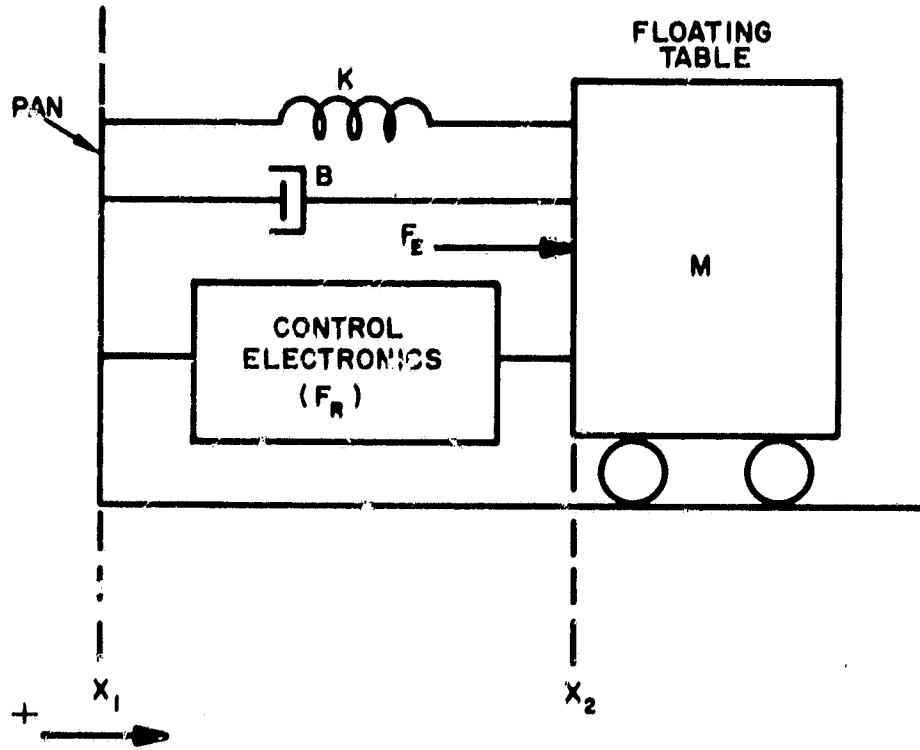
Fig. 5. Simplified model, single degree translation.

frame) of the floating portion of the thrust stand (called the table). The
damping and spring coefficients are denoted by B and K, respectively,
and F_R is the restoring control force which is of course proportional
to the difference between X_1 and X_2. F_E is the thruster force compo-
nent associated with the model and is to be determined for a knowledge
(measurement) of F_R. M denotes the total mass of the table and
thruster. Although the model is highly idealized, it is sufficiently realis-
tic to give considerable physical insight into the vibration problem and
indicates possible solutions.

It can be assumed that X_1 is a known quantity since it can be
derived from experimental measurements of the acceleration spectrum.
In an attempt to follow (with some simplification) the notation of the
previous quarterly report, let

$$F_E(S) = \frac{K_o M}{S} (S^2 + a_1 S + a_2)$$

$$G_M(S) = \frac{1/M}{S^2 + \frac{B}{M} S + \frac{K}{M}}$$

where

$$K_o = \left(\frac{P}{M}\right) \left(\frac{\delta E_x}{\delta_x}\right) K_D, \quad \text{rad/sec}$$

$$a_1 = K_p/K_D, \quad \text{rad/sec}$$

$$a_2 = K_I/K_D, \quad \text{rad/sec}^2$$

$$P \equiv \text{force motor gain, lb/V}$$

$$\frac{\delta E_x}{\delta_x} \equiv \text{displacement transducer gain, V/in.}$$

$K_p \equiv$ proportional gain, V/V

$K_D \equiv$ derivative gain, V-sec/V

$K_I \equiv$ integral gain, V/V-sec.

From Fig. 6 and the above notation, the block diagram shown in Fig. 7 can be developed. For $X_1 \equiv 0$ the configuration reduces to one discussed in the previous quarterly report. The effects of X_1 can be viewed equivalently as a disturbance force term which is superimposed on the thruster component F_E for a thrust stand in a vibration free environment. Therefore, Fig. 7 is an equivalent representation of the block diagram of Fig. 6 where the disturbance force F_V is given by

$$F_V(S) = [SB + K + G_E(S)] X_1(S)]$$
$$= G_V(S) X_1(S) .$$

Now assume that the compensation gains are adjusted such that

$$a_1 \simeq K_p/K_D = B/M$$
$$a_2 = K_I/K_D = K/M .$$

Then $G_V(S) = (\overline{K}_p + \overline{K}_D S + \overline{K}_I/S)$ where

$$\overline{K}_p = K_o B + K$$
$$\overline{K}_D = K_o M + B$$
$$\overline{K}_I = K_o K ;$$

hence F_V is the weighted sum of the integral, the derivative, and the scaled value of X_1.
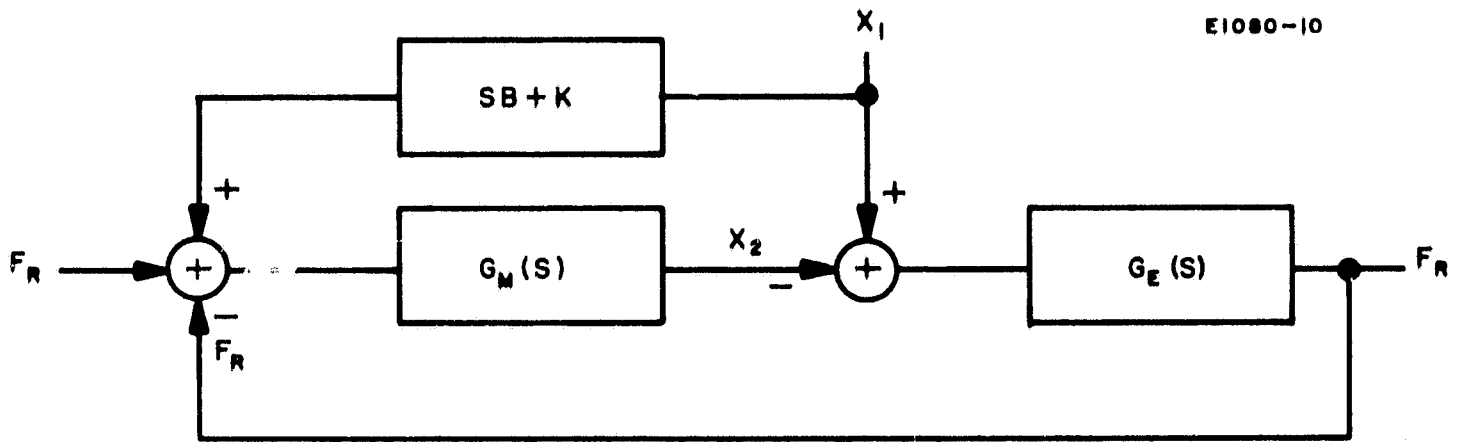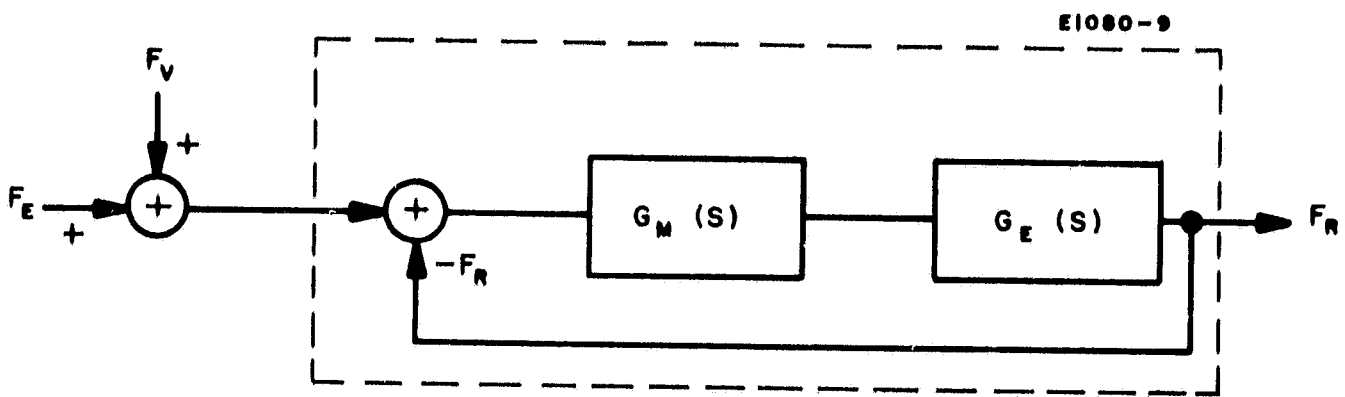
Fig. 6.   Block diagram of simplified model.

Fig. 7.   Equivalent block diagram of simplified model.

The closed loop transfer function becomes

$$G(S) = \frac{K_O}{S + K_O} = \frac{1}{S_T + 1} \; ; \quad \tau = \frac{1}{K_O} \quad .$$

Hence

$$F_R(S) = \frac{F_E(S)}{S_T + 1} + \frac{F_V(S)}{S_T + 1}$$

$$= F_{RE}(S) + F_{RV}(S) \quad .$$

If Z denotes the actual vibrational displacement of the support structure, then X_1 can be given by $Z(S) = A(S) \, X_1(S)$ where $A(S)$ represents the mechanical transfer function of the coupling to the thrust stand pan. F_{RV} is therefore

$$F_{RV}(S) = \left[\frac{(\overline{K}_p + \overline{K}_D S + \overline{K}_I/S) \, A(S)}{(S_T + 1)} \right] Z(S) \quad .$$

For the chosen model and values of gain coefficients the problem becomes one of determining F_{RE} from a measurement of F_R. The most attractive methods for obtaining accurate measurements of F_{RE} are to reduce F_V by isolating the thrust stand from the vibrating support structure (make $|A(S)| << 1$ for all frequencies of interest) or to separate F_{RE} from F_R by sufficient low pass filtering, or a combination of both of the above methods.

A vibration survey of the 9 ft vacuum chamber was performed. Various modes of chamber operation were investigated. Significant increases in vibration levels were observed during the operation of the holding pump for the chamber diffusion pump, at the initiation of the filling of the LN_2 cryowall, and the filling of the diffusion pump LN_2 baffle. Fortunately all three of these functions can be turned off manually during the thrust stand test and thus do not affect chamber vacuum performance. The significant result of the vibration survey was the

23

observation of an acceleration peak of 3×10^{-3} g occurring at 25 Hz. The frequency range is such that it may affect the thrust stand operation, imposing a background noise to the sensor which cannot be filtered out without affecting system response and sensitivity.

Vibration isolators in the form of air inflated cushions have resonance frequencies on the order of 1.5 Hz which could be employed to isolate the thrust stand platform from the chamber. However, because there is some concern about employing such a system within the vacuum chamber, other alternatives are being investigated. The most attractive alternative is the relocation and upending of a 4 ft chamber. It will be mounted on columns and a pneumatic vibration isolator will be located at the interface between the chamber and the column. Other equivalent vibration isolators will be located in the forepump and roughing pump lines. The isolators will be external to the vacuum chamber, so that the earlier problem of air leakage from the isolators into the vacuum will be eliminated. A preliminary sketch of the 4 ft diameter chamber in the upright position is shown in Fig. 8.

G.   Thrust Stand Design Summary

During the early part of this program the major emphasis has been on the design, fabrication, and test of the major components of the thrust stand. The detailed design of the over-all thrust stand is 90% complete; at this point the total "floated" weight of the thrust stand and the thruster system is required so that the center of gravity and the center of bouyancy may be determined and the counterweight assembly design may be completed.
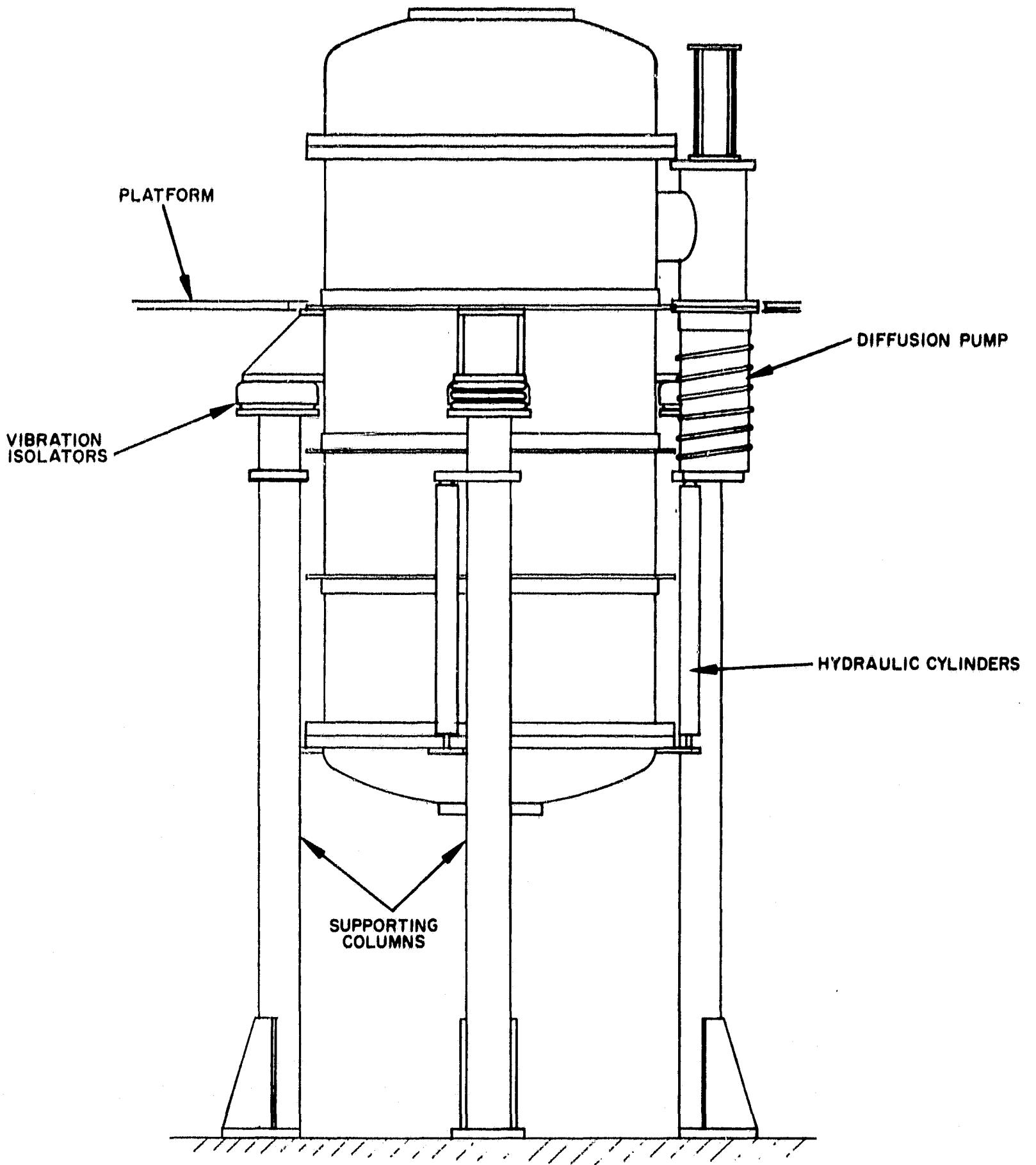
PLATFORM

DIFFUSION PUMP

VIBRATION
ISOLATORS

HYDRAULIC CYLINDERS

SUPPORTING
COLUMNS

Fig. 8. Preliminary sketch of the 4 ft diameter chamber in the up-
right position.

III. THRUSTER DESIGN

A 30 cm oxide cathode thruster designed and tested under a
HAC sponsored research program is used for this program. This
design is essentially a scaled up SERT II thruster, except that the
ionization chamber length was maintained at 15.2 cm in accordance
with the findings of Richley and Kerslake[3] and HRL contract
NAS 3-9703. Other modifications are the incorporation of a center
support between the accel and screen electrodes, and accel electrode
insulator supports attached through a double leaf spring arrangement
(as shown in Fig. 9) to absorb the bending torque which would be trans-
mitted to the screen electrode as a result of the differential in thermal
expansion. The propellant enters the ionization chamber through two
vapor lines, which feed into a manifold located within the chamber. The
propellant passes into the ionization chamber through twelve outlets
which are covered with a fine mesh screen. This configuration was em-
ployed to reduce the possibility of external leakage of the mercury vapor.
Leaks which might occur between the manifold and back plate would
remain within the ionization chamber and thus be less critical.

The thruster structure has been designed considering simple
sheet metal fabricating techniques in order to reduce thruster weight.
Thus, some of the complex structural configurations which might be
formed by spinning were formed from simple sheet configurations and
fusion heliarc welded to the desired configuration. For example, the
propellant manifold mentioned above could be formed by drawing or
spinning from a single sheet. It is a ring with a cross section shaped
like a squared off Greek letter capital omega, formed by rolling two
strips into hoops and adding three rings.

A.   Accel Electrode Support

The accel electrode support and insulator is shown in Fig. 9. The tang with the four holes in it is normally attached to the screen electrode. The cylindrical pieces in the center are the insulator shields; the insulator is completely shielded. The two flat vertical members shown to the left of the insulator are leaf springs. Another pair, one of which is visible in this sketch, is located on the right side. This support configuration was designed to provide flexibility between the accel and screen. Differential expansion between the accel and screen electrode will impart a minimum bending moment on the outer edges of the screen because the double springs will buckle equally and maintain the two interconnected mounting surfaces parallel. The accel electrode is mounted to the support assembly by the screw shown on the sketch. During the experimental portion of the program, the accel electrode will be displaced in incremental amounts laterally, rotationally, and axially. The support will then be inverted with the tang attached to a mounting ring. of the motion generator (described later) which encircles the thruster.

B.   Thruster Electrodes

The thruster electrodes were fabricated by an outside vendor by matched drilling on numerically controlled automatic tape drilling machines. Because they are match drilled they will index only one way. Our experience indicates that it is prohibitively expensive to make electrodes which are interchangeable and capable of being indexed along six axes. The electrode mount spacing is that which has been adopted for all of the 30 cm thrusters now being built at Hughes Research Laboratories. The screen electrode is 0.030 in. thick and the openings are 0.188 in. in diameter. The center-to-center spacing is 0.211 in. resulting in an open area of 72.2%. The accel electrode openings are 0.140 in. in diameter with an open area of 40.5%. The accel electrode is 0.100 in. thick.
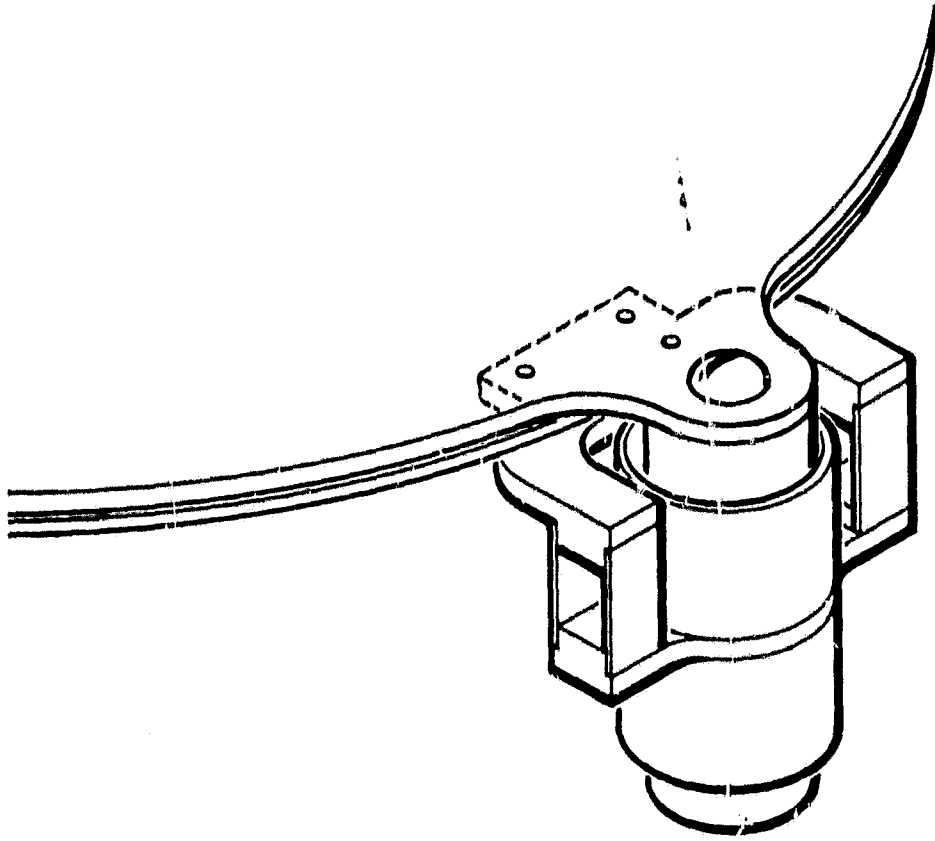
E1010-15R1

Fig. 9.   Accel support and insulator.

The material specified for the electrodes is arc-cast molybdenum. The material as received from the producer was annealed at 1650°F (900°C) for 1 hour. A 0.020 in. bow was observed in the screen electrode and a 0.004 in. bow was observed in the accel electrode after machining. The electrodes were fixtured between two Blanchard ground steel plates to be stress relieved and flattened at 900°C in a vacuum furnace for 1 hour. The fixture consisted of two heavy (125 lb each) Blanchard ground steel plates coated with a 5% weight solution of Baymal in water as an antiseizing agent. A 0.005 in. thick molybdenum sheet coated on both surfaces with Baymal was placed between the plates and the electrodes and between the electrodes. The electrodes were also coated on both sides. The antiseizing agent and the thin molybdenum sheets were used to prevent "cold" welding in vacuum. The interface between molybdenum pieces probably would not be subject to "cold" welding at this temperature but the steel plates will without the antiseizing coating.

After stress relieving and flattening, the electrodes were flat within 0.002 in. over their entire surface.

C.   Center Support

A drawing of the center support is shown in Fig. 10. It projects into the upstream or ionization chamber side of the electrodes. A minimum cone shaped nut is placed in the downstream or beam side to reduce the possibility of beam interception. The cup is attached to the screen electrode by a 90° included angle cone shaped shoulder on the bushing which screws into the cup, through a matching countersunk center hole in the screen electrode. The end of the bushing fits flush with the surface of the screen electrode. The insulator fits freely in the cup and bushing and is attached to the bottom of the cup. Threaded end fittings are swaged over the ends of the solid alumina rod insulator. In addition to being a mount for one end of the insulator, the cup also acts as a shield from surface contamination. The other threaded end fitting of the insulator passes through a clearance in the accel electrode hole and is held by the cone shaped cap. The metal parts of the center support are fabricated of tantalum because of its elevated temperature properties and room temperature ductility.
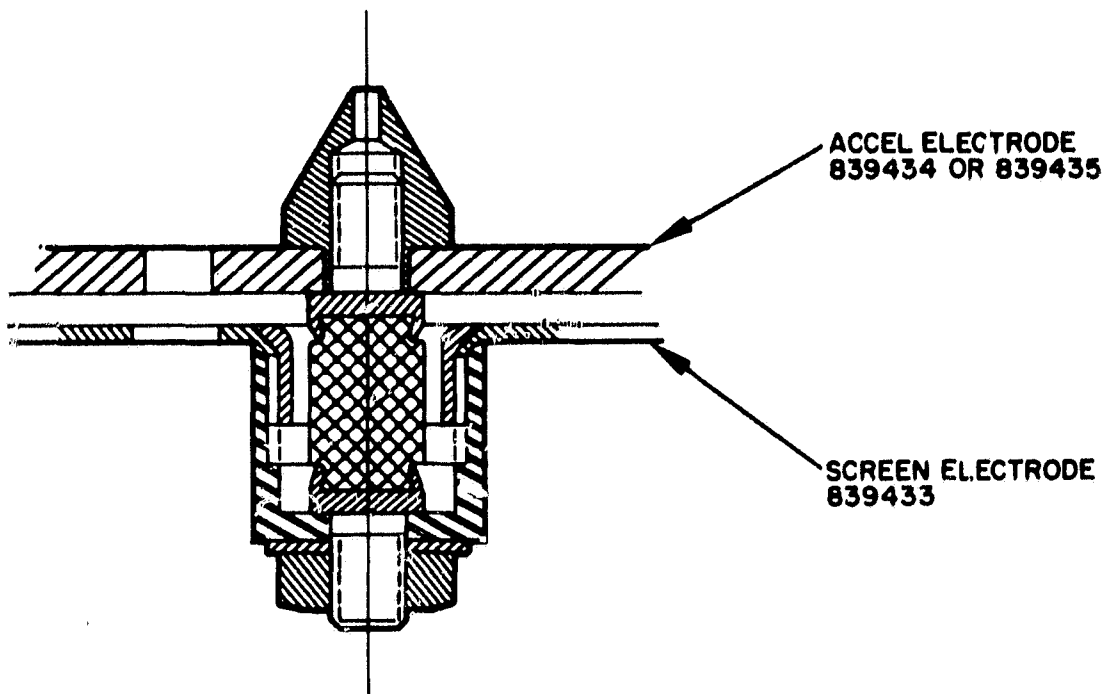
Fig. 10.   Center support.

D.   Accel Electrode Motion Generator and Monitor

To effect the electrode displacement predicted and analyzed in Phase I of this program, a mechanism is required which will move the accel electrode axially, laterally, and rotationally, and also tilt the accel with respect to the screen in varying amounts. A mechanism for these motions would require the capability of producing the small motions repeatedly. (Total excursions: 0.020 in. axially, axial tilt, laterally and rotationally at the outer bounding opening of the accel electrode.) A system employing three solenoid driven stepper motors with a cam actuator for axial motion was described in the previous quarterly. With such a system the greatest problem would be to obtain exact operation of each motion generator.

A spring column system has been designed which will operate with one stepper motor. This system is shown in Fig. 11. The motion generator base platform is attached directly to the floating sensor force motor platform. The thruster is mounted to this base platform. Eight leaf spring columns are attached around the periphery of this base platform, with each column slightly buckled radially inward. The columns are held in the buckled attitude by two cables each passing over sheaves attached to the centers of four columns. The cables are attached to the shaft of a stepper motor through an eccentric arm. Rotation of the shaft of the stepper motor results in shortening of the cable, causing the column to buckle more and reducing the axial separation of the accel from the screen electrode. A 180° rotation or six pulses of the stepper motor produces the maximum axial motion. Another 180° returns the accel electrode to its original position.

As mentioned above two lengths of cable are employed, each working on four columns. One end of the cable is fixed to the platform. The other end of the cable is attached to an eccentric on the shaft of a second stepper motor. Actuation of this stepper motor will cause the four columns on that cable to buckle, resulting in tilting of the accel electrode with respect to the screen electrode.
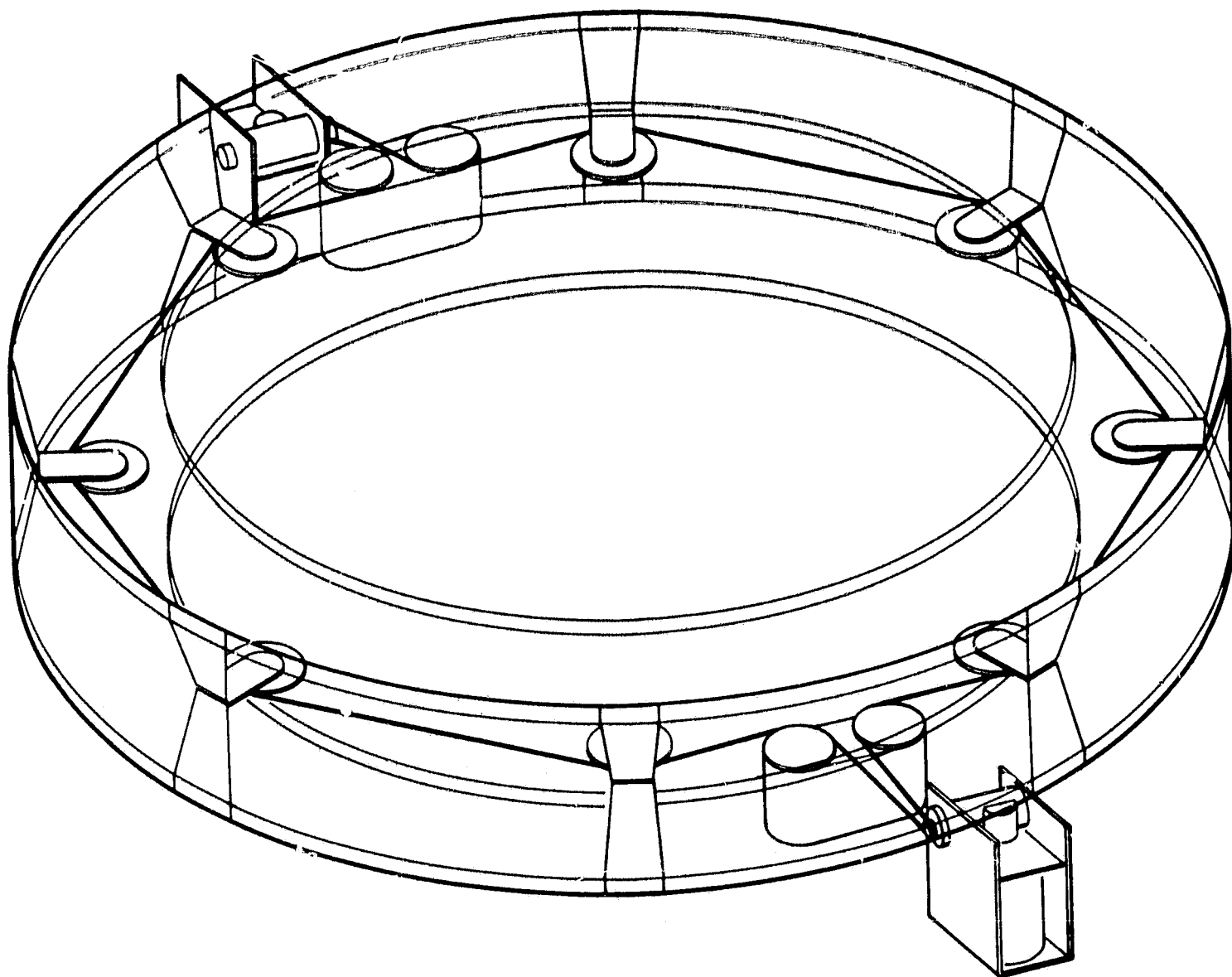
Fig. 11.   Spring column system.

This motion generator system is now being fabricated. The stepper motor used is a commercial solenoid operated ratchet device. Each actuation produces a 30° rotation of the shaft. Six inch ounces of torque is available at the shaft. For a total eccentric excursion of 0.20 in. or 0.10 in. arm length, 60 oz of force is available. A similar stepper motor was designed at HRL, with an overrunning clutch drive instead of the ratchet drive. The overrunning clutch is a commercially available unit which became erratic in operation after 30,000 cycles at 130°C. The major problem appears to be the use of plastic carriers for the clutch rollers. This design was discarded in favor of the positive ratchet drive.

A third plate is employed for the electrode lateral and rotational displacement. This third plate is positioned on the axial plate and is displaced by a third and fourth stepper motors. The displacement is produced by a cam operating in properly oriented cam followers. The cam followers consist of two plates with elongated holes. Two plates are used to provide a simple adjustment of the follower to the cam.

The motion monitor is a commercially produced induction transformer. Tests of this device have shown that the best sensitivity is obtained at 400 Hz into the primary coil. The sensitivity obtained was in the 1.5 mV output/V-input 0.001. The device is not sensitive to radial displacement of the movable core, nor do elevated temperatures to 130°C affect its sensitivity. One monitor will indicate the axial position of the accel electrode and second will be positioned to sense its lateral and radial displacement.

Measurement of the electrode surface contours during thruster operation was described in the previous quarterly report. The pins and alignment telescope were used on a bench thermal test of the screen and accel electrode.

34

E.   Electrode Thermal Tests

Three thermal bench tests were performed to simulate the thermal load on the electrodes. The first and second tests were performed with only the screen electrodes; in the first the screen electrode was mounted with the edges free except at one point. The thermal gradient across the face of the electrode was maintained at approximately $33^{\circ}C$. The second test was performed with the screen electrode and the edges clamped. The third test was performed with the accel electrode in place, the center support attached, and the screen electrode edges free except at one point.

The main mounting of the electrode was the screen collar of the thruster structure, which was supported by three machinists angle plates positioned on a large granite surface plate. A screen pole piece was attached to the collar and the screen electrode was placed on top of it exactly as it would be on the thruster. The assembly was leveled by placing a groundgauge block on the screen electrode near each angle plate support and checking its height on the alignment scope. A circular concentric three element electrical heater was located about 4 in. below the screen electrode. A cylindrical radiation shield of approximately the diameter of the anode was placed around the heater and extended toward but not touc' 'ng the electrode. Each of the three elements was separately controlled through a variac.

The results of these tests are shown in Figs. 12 through 14. Figures 12 through 14 show · the difference between the heights of the ends of screws attached to the screen electrode along three diameters for tests 1 through 3. Figure 15 shows the height of a reference block of tungsten placed adjacent to the screws protruding through the openings in the accel electrode in test 3. The figures show a "potato chip" unstable effect of thermal loading on "flat" plates. The electrodes were stress relieved and flattened before the tests were set up. In
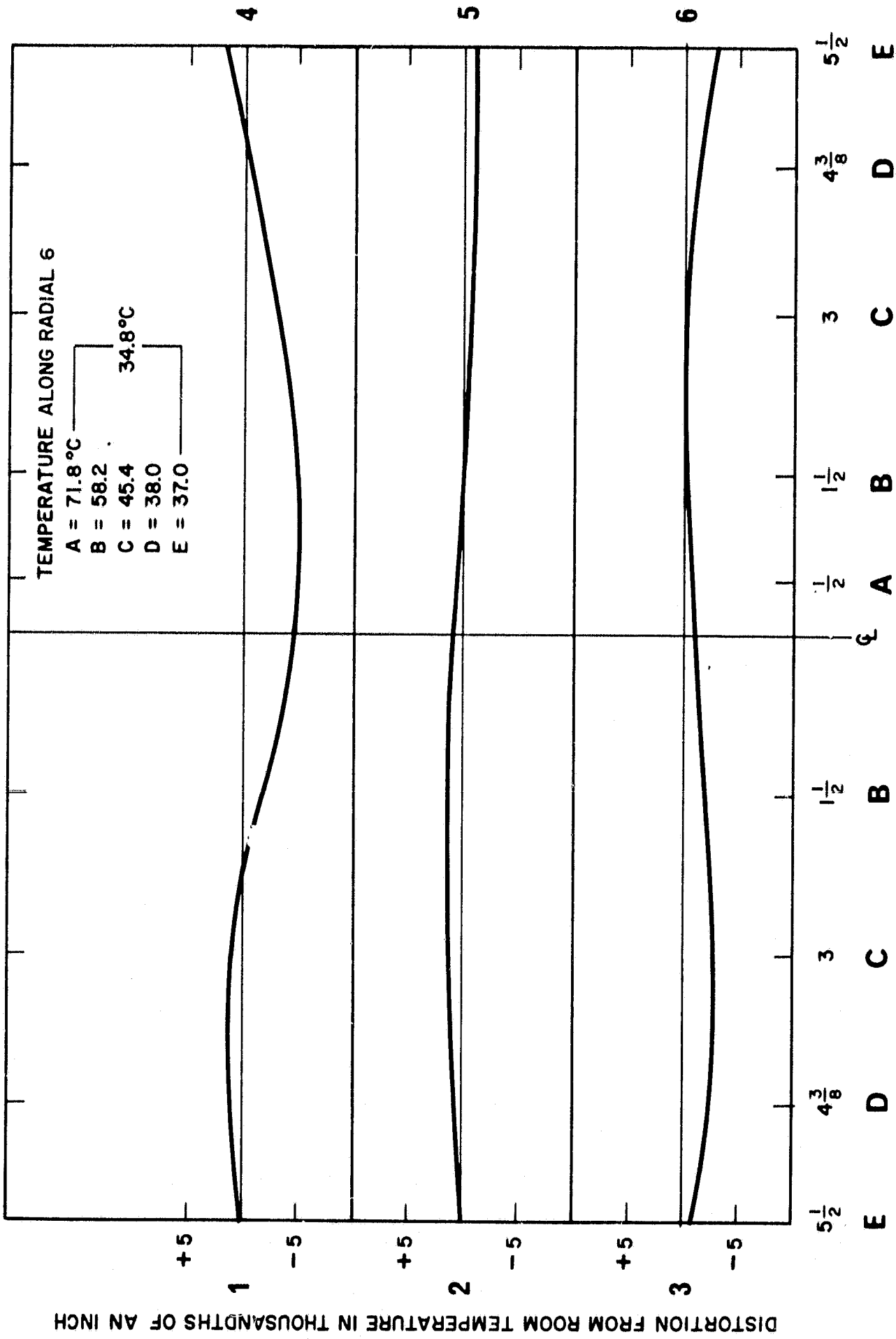
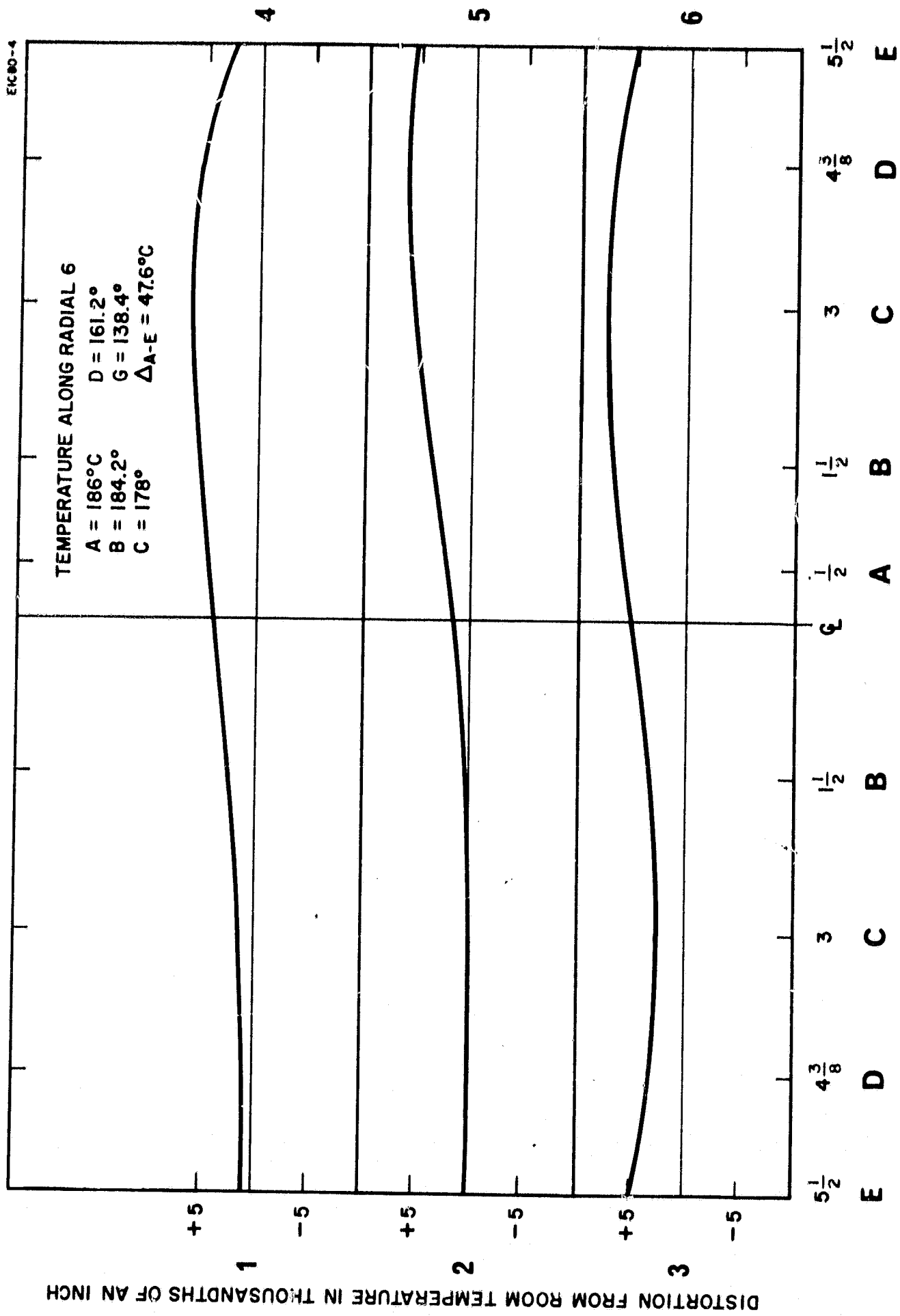Fig. 12.   Screen electrode thermal deformation.

TEMPERATURE ALONG RADIAL 6

A = 71.8°C
B = 58.2
C = 45.4   34.8°C
D = 38.0
E = 37.0

DISTORTION FROM ROOM TEMPERATURE IN THOUSANDTHS OF AN INCH

E1080-6

36

Fig. 13.   Screen electrode thermal deformation.

37

TEMPERATURE ALONG RADIAL 6

A = 186°C   D = 161.2°
B = 184.2°   G = 138.4°
C = 178° Δ_{A-E} = 47.6°C

Fig. 14.   Screen electrode thermal deformation.

DISTORTION FROM ROOM TEMPERATURE IN THOUSANDTHS OF AN INCH

EK80-4

Fig. 15. Accel electrode thermal deformation.

setting up the test the electrodes were heated and handled and may
have been subjected to high localized stresses which were suffi-
cient to initiate local distortions of varying magnitude and direction.

After the tests were completed the electrodes were inspected
for any deformation that might have occurred. A deformation of
4 mils was measured in the accel and 12 mils in the screen.

IV. THRUSTER TEST RESULTS

The thruster was installed in the 9 ft chamber and tested. The first test performed with eight 13/64 x 25/64 in. rectangular cross section permanent magnets showed a discharge instability which was attributed to a high magnetic field. Higher than normal accelerator drains were also observed, but they were later attributed to misalignment of the electrodes. The engine was removed and two of the eight magnets removed. The alignment of the accel electrode to the screen electrode was checked and corrected and the thruster was reinstalled in the chamber.

Because of the increased spacing between the magnets, the azimuthal variations in magnetic field increased to the point that intensity variations in the discharge plasma could be observed visually. The thruster performance was erratic and relatively poor.

The permanent magnets were replaced with twelve electromagnets and the thruster was again tested. With this configuration the thruster was operated at 1 A of beam current at a propellant utilization efficiency of 80% and an ion chamber performance of about 200 eV/ion. Ten permanent magnets with a cross section of 9/64 by 25/64 in. were installed and stable operation at beam currents ranging from 900 to 1400 mA was measured at accel drains of 0.4 to 0.5%. The discharge chamber performance during this test was 220 eV/ion at a mass utilization of 85 ± 5% the accelerator and screen temperatures measured during this run at the periphery of the electrodes were 225°C and 228°C, respectively.

V.   CONCLUSIONS

The conclusions from the work performed during this quarter are listed below.

Tests of a breadboard force motor-sensor loop indicate sufficient sensitivity and gain to measure thrust on the order of 10^{-4} lb. The effects of external excitations (i. e., vibration) should be isolated mechanically so that accurate measurements may be obtained. A 4 ft diameter chamber is being relocated and mounted on vibration isolators.

Thruster performance will meet the specified propellant utilization efficiency by the selection of the proper number and size of the permanent magnets.

Thrust stand design and fabrication is approximately 80% complete.

VI. WORK TO BE ACCOMPLISHED

The following tasks remain to be accomplished.

1. Thruster test with more permanent magnets of a smaller cross section. Thruster test with accel electrode motion generators.

2. Complete thrust stand design: Determine floating weight, design counterweight mechanism, design feed system reservoir and heater. Assemble thrust stand and bench test.

3. Integrate thruster and thrust stand. Perform evaluation tests of integrated system.

REFERENCES

1. Dow Corning Product Brochure, Engineering Applications of Silicone Rubber, 1963.

2. M. Morton, Introduction to Rubber Technology, Reinhold, New York, 1959.

3. E. A. Richley and W. R. Kerslake, "Bombardment Thruster Investigations at the Lewis Research Center," AIAA Paper No. 68-542, presented at AIAA 4th Propulsion Joint Specialist Conference, Cleveland, Ohio, June 1968.